Surface-to-surface registration using level sets

Mads Fogtmann Hansen[1], Søren Erbou[1], Martin Vester-Christensen[1], Rasmus Larsen[1], Bjarne Ersbøll[1], and Lars Bager Christensen[2]

[1] Technical University of Denmark
[2] Danish Meat Research Institute

Abstract. This paper presents a general approach for surface-to-surface registration (S2SR) with the Euclidian metric using signed distance maps. In addition, the method is symmetric such that the registration of a shape A to a shape B is identical to the registration of the shape B to the shape A.

The S2SR problem can be approximated by the image registration (IR) problem of the signed distance maps (SDMs) of the surfaces confined to some narrow band. By shrinking the narrow bands around the zero level sets the solution to the IR problem converges towards the S2SR problem. It is our hypothesis that this approach is more robust and less prone to fall into local minima than ordinary surface-to-surface registration. The IR problem is solved using the inverse compositional algorithm.

In the paper a set of 40 pelvic bones of Duroc pigs are registered to each other with respect to the Euclidean transformation with both the S2SR approach and iterative closest point approach. The results of the two registration methods are compared both visually and with quality measures.

1 Introduction

This paper addresses the problem of shape registration or alignment which plays an essential role in shape analysis. Many registration proceduces such generalized Procrustes analysis [7, 3] rely on a prior manual annotation of landmarks. The main drawback with these approaches is the reliance on manual annotation which becomes cumbersome and infeasible for larger 2D datasets and for 3D data.

The iterative closest point (ICP) algorithm by Besl et al. [2] solves the problem of landmark dependence by iteratively updating the point correspondence after the closest point criterium. Since the introduction in 1992 numerous extension and improvements of original ICP has proposed in literature [5, 8, 6]. Most of these methods still require a good initial estimate in order not to converge to a local minimum. Furthermore, common for these methods are that they do not utilize the knowledge of the connectedness of the point cloud, which is available in many cases.

The approach described in this paper is in many ways related to the approach presented by Darkner et al. [4], which aligns two point clouds by minimizing the squared difference between the distance functions of the point clouds in some rectangular box domain. Our approach differentiatea itself from the approach presented in [4], as it uses *signed* distance maps and minimizes the squared difference between the signed distance maps restricted to a shrinking narrow band.

2 Theory

The registration of a surface S_x to a surface S_y w.r.t the Euclidian metric can be expressed as the minimization of the functional

$$F_1(\boldsymbol{p}) = \oint_{\mathcal{S}_x} d(W(\boldsymbol{x};\boldsymbol{p}), \mathcal{S}_y)^2 d\boldsymbol{x}, \tag{1}$$

where $W(\_;\boldsymbol{p})$ is the warp function.
A minor flaw with this approach is that registration of S_x to S_y is not necessarily equivalent to the registration S_y to S_x. If $W(\_;\boldsymbol{p})$ is invertible (1) can be extended to

$$\begin{aligned} F_2(\boldsymbol{p}) &= \oint_{\mathcal{S}_x} d(W(\boldsymbol{x};\boldsymbol{p}), \mathcal{S}_y)^2 d\boldsymbol{x} + \oint_{\mathcal{S}_y} d(W(\boldsymbol{y};\boldsymbol{p})^{-1}, \mathcal{S}_x)^2 d\boldsymbol{y} \\ &= \oint_{\mathcal{S}_x} d_{,\mathcal{S}_y}(W(\boldsymbol{x};\boldsymbol{p}))^2 d\boldsymbol{x} + \oint_{\mathcal{S}_y} d_{\mathcal{S}_x}(W(\boldsymbol{y};\boldsymbol{p})^{-1})^2 d\boldsymbol{y}, \end{aligned} \tag{2}$$

where $d_{\mathcal{S}_x}$ and $d_{\mathcal{S}_y}$ are the distance map functions of the surfaces $\mathcal{S}_x$ and $\mathcal{S}_y$. This energy functional ensures a symmetric registration.
A minimum of (2) can be obtained by any gradient or Newton based optimization scheme. However, such schemes may very well get stuck in a local minimum instead of the global minimum. To overcome this problem we introduce a slightly different energy functional

$$F_3 = \int_{U_x^r} (\Phi_y(W(\boldsymbol{x};\boldsymbol{p})) - \Phi_x(x))^2 d\boldsymbol{x} + \int_{U_y^r} (\Phi_x(W(\boldsymbol{y};\boldsymbol{p})^{-1}) - \Phi_y(y))^2 d\boldsymbol{y}, \tag{3}$$

where $\Phi_x(\boldsymbol{x})$ and $\Phi_y(\boldsymbol{y})$ are the SDM functions of the surfaces $\mathcal{S}_x$ and $\mathcal{S}_y$, and $U_x^r = \{\boldsymbol{x} \mid \boldsymbol{x} \in \mathbb{R}^d, |\Phi(x)| < r\}$. And we note that

$$F_3 \rightarrow F_2 \text{ for } r \rightarrow 0. \tag{4}$$

Now, consider the shape in Figure 1 consisting of two identical rectangles. If we translate the shape in both the x and the y direction between -25 and 25 pixels and calculate the energy in each position using (2) and (3) with $r = 25$ pixels we get energy landscapes shown in Figure 2. In this case, the (2) cost function produces three minima while the (3) cost function produces only the global minimum.

Unfortunately, SDM's are in principal only defined for closed curves and surfaces. In the Experiment section of this paper, we will however demonstrate how one can define a kind of pseudo SDM for open curves and surfaces.

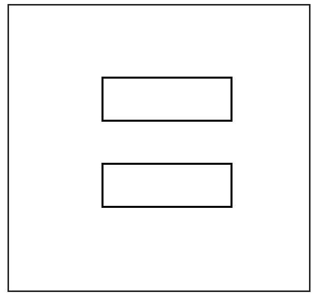

Fig. 1. A simple shape.

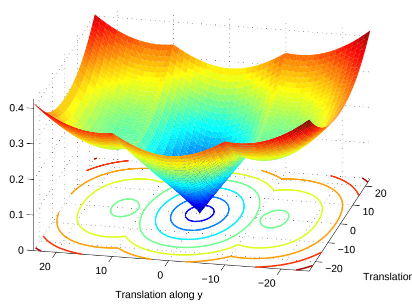

(a) F_2 cost functional.

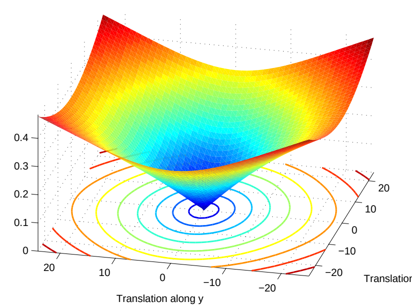

(b) F_3 cost functional.

Fig. 2. Cost as a function of translation in x and y direction.

3 Method

The energy functional defined in (3) can be viewed as a image registration problem between two SDM's Φ_x and Φ_y, where the points to be warped are those inside the narrow bands U_x^r and U_y^r. The problem is solved using an extended version of the inverse compositional algorithm presented by Baker et al [1]. To preserve the same notation as in [1], we assume that Φ_x and Φ_y are discretized signed distance functions. Thus, (3) becomes

$$F_4 = \sum_{\boldsymbol{x} \in U_x^r} (\Phi_y(W(\boldsymbol{x};\boldsymbol{p})) - \Phi_x(\boldsymbol{x}))^2 + \sum_{\boldsymbol{y} \in U_y^r} (\Phi_x(W(\boldsymbol{y};\boldsymbol{p})^{-1}) - \Phi_y(\boldsymbol{y}))^2. \qquad (5)$$

If the set of warps forms a *group* the minimization of (5) is equivalent to the minimization of

$$\begin{aligned} F_5 = &\sum_{\boldsymbol{x} \in U_x^r} (\Phi_y(W(\boldsymbol{x};\boldsymbol{p})) - \Phi_x(W(\boldsymbol{x};\Delta\boldsymbol{p})))^2 \\ &+ \sum_{\boldsymbol{y} \in U_y^r} (\Phi_x(W(\boldsymbol{y};\boldsymbol{p})^{-1}) - \Phi_y(W(\boldsymbol{y};\Delta\boldsymbol{p})^{-1}))^2. \end{aligned} \qquad (6)$$

with the update rule $W(\boldsymbol{x};\boldsymbol{p}) \leftarrow W(\boldsymbol{x};\boldsymbol{p}) \circ W(\boldsymbol{x};\Delta\boldsymbol{p})^{-1}$. By applying the first order Taylor expansion to (6) we get

$$\begin{aligned} F_5 \approx &\sum_{\boldsymbol{x} \in U_x^r} \left(\Phi_y(W(\boldsymbol{x};\boldsymbol{p})) - \Phi_x(W(\boldsymbol{x};\boldsymbol{0})) - \nabla\Phi_x \frac{\partial W}{\partial \boldsymbol{p}} \Delta\boldsymbol{p}\right)^2 \\ &+ \sum_{\boldsymbol{y} \in U_y^r} \left(\Phi_x(W(\boldsymbol{y};\boldsymbol{p})^{-1}) - \Phi_y(W(\boldsymbol{y};\boldsymbol{0})^{-1}) - \nabla\Phi_y \frac{\partial W^{-1}}{\partial \boldsymbol{p}} \Delta\boldsymbol{p}\right)^2. \end{aligned} \qquad (7)$$

By taking the derivatives of (7) w.r.t $\Delta\boldsymbol{p}$ and setting them equal to zero we get the update equation

$$\Delta\boldsymbol{p} = -\boldsymbol{H}^{-1} \left(\sum_{\boldsymbol{x} \in U_x^r} \boldsymbol{S}_x^\top (\Phi_y(W(\boldsymbol{x};\boldsymbol{p})) - \Phi_x(\boldsymbol{x})) + \sum_{\boldsymbol{y} \in U_y^r} \boldsymbol{S}_y^\top (\Phi_x(W(\boldsymbol{y};\boldsymbol{p})^{-1}) - \Phi_y(\boldsymbol{y})) \right), \qquad (8)$$

where $\boldsymbol{S}_x = \nabla\Phi_x \frac{\partial W}{\partial \boldsymbol{p}}$, $\boldsymbol{S}_y = \nabla\Phi_y \frac{\partial W^{-1}}{\partial \boldsymbol{p}}$ and $\boldsymbol{H} = \boldsymbol{S}_x^\top \boldsymbol{S}_x + \boldsymbol{S}_y^\top \boldsymbol{S}_y$.

A S2SR can be obtained with Algorithm 1.

We suggest you use the following scheme for selecting an appropriate sequence of r_i's:

$$r_{i+1} = \frac{r_i}{2}. \qquad (9)$$

It is however more tricky to choose the best r_0. So far, we have not been able to find a bullet proof way of choosing an appropriate initial narrow band. Essentially, it has to be large enough!

Algorithm 1 S2SR

$\boldsymbol{r} = [r_1 \dots r_n]$; $\{ r_i > r_{i+1} \}$
for each $r_i \in \boldsymbol{r}$ **do**
  $k = 0$;
  repeat
    update $\boldsymbol{p}$ using (8) with $U_x^{r_i}$ and $U_y^{r_i}$;
    $k = k + 1$;
  until *convergence* or $k > k_{max}$
end for

4 Experiments

Two experiments were conducted to test the surface registration approach ; (i) a toy example where the outline of the right and left hand of one of the authors were registered to each other, and (ii) a real example where 40 pelvic bones of Duroc pigs are registered with the ICP algorithm by Fitzgibbon [5] and with our S2SR algorithm.

4.1 Hand example

To test the robustness of the S2SR algorithm a left and a right and hand were traced on a piece of paper and scanned into a computer. The left hand was flipped horizontally, displaced 100 pixels in the x-direction and -25 pixels in the y-direction, and rotated 5 degrees counter clockwise. Figure 3 shows the initial position of the hands, the final position with regular S2SR[3] and last the final position with our S2SR algorithm with the narrow bands $r = 30,\ 15,\ 1$. Evidently, the regular S2SR approach gets stuck in a local minimum or saddle point, while the shrinking narrow band S2SR approach registers the left and right hand perfectly.

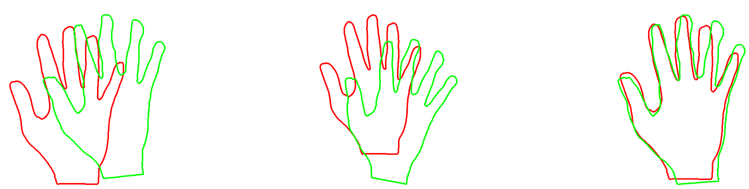

(a) Initial position. (b) Final position for S2SR with narrow band r=1. (c) Final position for S2SR with narrow bands 30, 15, 1.

Fig. 3. Rigid registration of left (green) and right hand (red).

[3] Simulated with the small narrow band r=1.

4.2 Pelvic bones

Half pig skeletons were automatic extracted from CT scans of half pig carcasses and fitted with implicit surfaces. From the implicit surfaces triangle meshes were created, and the pelvic bones were manually removed from the triangulated skeletons. An example of a pelvic bone can be found in Figure 4. One problem with the triangulated pelvic bones is that they are open surfaces, and thus cannot be converted to SDM's. As a work around the triangle meshes were closed by triangulating the open parts and then converted to discretized SDM's. Hereafter, all voxels in the discretized SDM's with distances to the added faces were set to an undefined value. Consequently, under the registration voxels from one SDM may be warped to an undefined area of the other SDM. In such cases, the distance in the undefined area is assumed to be 0. This hack is actually reasonable as it gives a bit of slack around the open areas of a surface. In many cases a surface is only open as it has been chosen to disregard part of the shape - cutting away part of a shape in the exact *same place* is impossible.

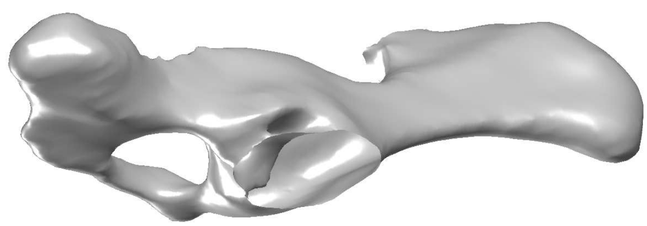

Fig. 4. Example of a pelvic bone from a Duroc pig.

From the set of pelvic bone shapes a shape was selected randomly to be the reference, and the remaining shapes were registered to the reference shape with ICP and our level set based S2SR algorithm with $r = 20mm$, $10mm$, $5mm$, $1mm$. To compare the two registration approaches we use the mean squared error (MSE) and the maximum error (ME). As ICP minimizes the point-to-closest-point (CP) distance and our algorithm minimizes the surface-to-surface distance[4] we evaluate the performance of registration algorithms using both distance concepts. Furthermore, as our registration algorithm does symmetric minimization of the squared distances and ICP does not, the MSE and the ME are calculated in the same direction as the ICP registration, in the other direction and both

[4] The distances are found by interpolating the SDMs. To ensure fairness, when evaluating the MSE and ME, points, which are warped to an undefined area of a SDM, are ignored instead of receiving the distance 0.

directions combined. The results of the registration are shown in Table 1. As no surprise, the ICP registration has a lower MSE and ME in the same direction as the registration, when we are using the CP distance. It is neither a surprise that our S2SR algorithm has lower MSEs and MEs in the opposite direction of the ICP registration and in both directions. It is however a bit of a surprise, that our S2SR algorithm has a smaller MSE than ICP when using SDMs to extract distances. A possible reason for this result is that our algorithm allows for a bit of slack around the open regions of the surface, and is therefore better at fitting the remaining regions of the surface. Figure 5 illustrates this by color-coding the surface of a pelvic with the shortest distance.

Method	ICP ($A \rightarrow B$)						S2SR ($A \leftrightarrow B$)					
Direction	$A \rightarrow B$		$A \leftarrow B$		$A \leftrightarrow B$		$A \rightarrow B$		$A \leftarrow B$		$A \leftrightarrow B$	
Measure	$\sqrt{MSE}$	ME	$\sqrt{MSE}$	ME	$\sqrt{MSE}$	ME	$\sqrt{MSE}$	ME	$\sqrt{MSE}$	ME	$\sqrt{MSE}$	ME
SDM	11.92	20.13	12.70	27.04	12.34	27.24	11.69	24.11	12.18	24.03	11.90	26.28
CP	12.32	20.85	14.40	29.41	13.44	29.48	12.77	25.70	13.11	26.34	12.95	28.30

Table 1. The MSE and ME averaged over the 39 registrations (in mm) after registration.

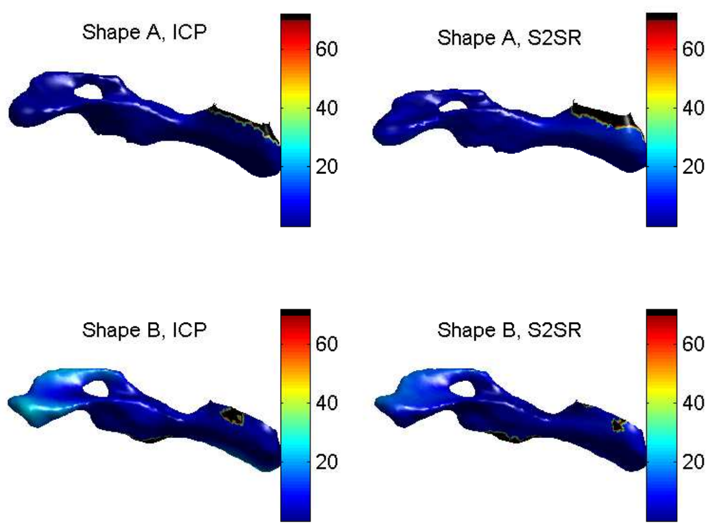

Fig. 5. Distance color-coded surfaces after registration. Black areas are areas where the distance could not be interpolated in the SDM because the point is situated in a undefined area.

5 Conclusion

This paper presented a method for S2SR. The registration algorithm was tested on two examples, where its properties were highlighted; (i) it is less prone to fall into local minima than ordinary S2SR, (ii) and it does symmetric registration. As the method relies on SDMs it only works in theory on closed curves and surfaces. Nevertheless, this paper demonstrated that it can work on open surfaces by introducing a pseudo SDM, where distances are not defined in regions *close* to the open areas of the surface. In the future, we will use non-rigid transformation with the registration approach.
With regards to computation time, it can be mentioned that it took a little less than 50 minutes to run 39 pelvic bone registrations on a standard Dell laptop with a 1.6Ghz Centrino CPU and 2Gb ram.

References

1. S. Baker, I. Matthews. "Lucas-Kanade 20 Years On: A unifying Framework". *CMU*. Part 1, 2002.
2. P. J. Besl, N. D. Mckay. "A Method for Registration of 3-D Shapes". *IEEE Transaction on Pattern Analysis and Machine Intelligence* . Vol. 14, p. 239-256, 1992.
3. I.L. Dryden, K.V. Mardia, "Statistical Shape Analysis",*John Wiley*, 1998
4. S. Darkner, M. Vester-Christensen, R. Larsen, C. Nielsen, R. R. Paulsen, "Automated 3D Rigid Registration of Open 2D Manifolds", *MICCAI 2006 Workshop "From Statistical Atlases to Personalized Models"*, 2006.
5. A. Fitzgibbon. "Robust Registration of 2D and 3D Point Sets". *In Proc. British Machine Vision Conference*. Vol. II, 2001.
6. S. Granger, X. Pennec. "Multi-scale EM-ICP: A Fast and Robust Approach for Surface Registration." *ECCV 2002*, 2002.
7. J. C. Gower. "Generalized procrustes analysis". *Psychometrika*, 1975.
8. S. Rusinkiewicz, M. Levoy. "Efficient Variants of the ICP Algorithm. *3DIM 2001*,2001.